Science of the Total Environment 771 (2021) 145384

Contents lists available at ScienceDirect

Science of the Total Environment

journal homepage: www.elsevier.com/locate/scitotenv

Mapping soil organic carbon stocks and trends with satellite-driven high resolution maps over South Africa

Zander S. Venter [a,b,*], Heidi-Jayne Hawkins [c,d], Michael D. Cramer [d], Anthony J. Mills [e]

[a] Terrestrial Ecology Section, Norwegian Institute for Nature Research - NINA, 0349 Oslo, Norway
[b] ZSV Consulting, Unit 104, Sunstone, Ruby Estate, Marquise Drive, Burgundy Estate, South Africa
[c] Conservation South Africa, 301 Heritage House, 20 Dreyer Street, 7735, Claremont, Cape Town, South Africa
[d] Department of Biological Sciences, University of Cape Town, Private Bag X1, 7701, Rondebosch, Cape Town, South Africa
[e] C4 EcoSolutions, 18 Gerrie Avenue, Dennendal, 7945 Cape Town, South Africa

HIGHLIGHTS

- First national-scale map of soil organic carbon (SOC) stocks and trends for South Africa at 30 m resolution
- Machine learning workflow using three decades of satellite imagery
- Total SOC stock of 5.6 Pg C in natural areas of South Africa
- Net sequestration of SOC between 1984 and 2019 in natural areas
- Both increased and decreased SOC may be associated with habitat loss.

GRAPHICAL ABSTRACT

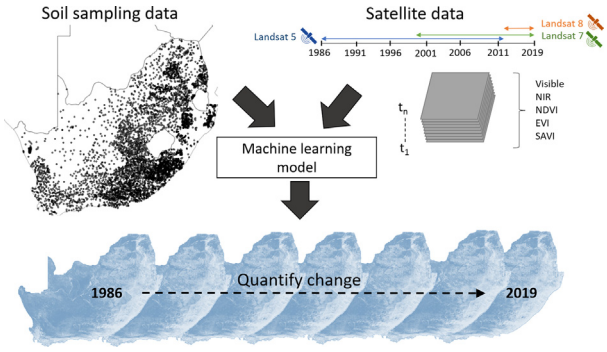

ARTICLE INFO

Article history:
Received 3 November 2020
Received in revised form 30 December 2020
Accepted 19 January 2021
Available online 27 January 2021

Editor: Dr. Jay Gan

Keywords:
Carbon stocks
Land degradation
Natural climate solutions
Remote sensing
Soil mapping
Spatial prediction

ABSTRACT

Estimation and monitoring of soil organic carbon (SOC) stocks is important for maintaining soil productivity and meeting climate change mitigation targets. Current global SOC maps do not provide enough detail for landscape-scale decision making, and do not allow for tracking carbon sequestration or loss over time. Using an optical satellite-driven machine learning workflow, we mapped SOC stocks (topsoil; 0 to 30 cm) under natural vegetation (86% of land area) over South Africa at 30 m spatial resolution between 1984 and 2019. We estimate a total topsoil SOC stock of 5.6 Pg C with a median SOC density of 6 kg C m^{-2} (IQR: interquartile range 2.9 kg C m^{-2}). Over 35 years, predicted SOC underwent a net increase of 0.3% (relative to long-term mean) with the greatest net increases (1.7%) and decreases (−0.6%) occurring in the Grassland and Nama Karoo biomes, respectively. At the landscape scale, SOC changes of up to 25% were evident in some locations, as evidenced from fence-line contrasts, and were likely due to local management effects (e.g. woody encroachment associated with increased SOC and overgrazing associated with decreased SOC). Our SOC mapping approach exhibited lower uncertainty ($R^2 = 0.64$; $RMSE = 2.5$ kg C m^{-2}) and less bias compared to previous low-resolution (250–1000 m) national SOC mapping efforts (average $R^2 = 0.24$; $RMSE = 3.7$ kg C m^{-2}). Our trend map remains an estimate, pending repeated measures of soil samples in the same location (time-series); a global priority for tracking SOC changes. While high resolution SOC maps can inform land management decisions aimed at climate mitigation (natural climate solutions), potential increases in SOC are likely limited by local climate and soils. It is also important that climate mitigation efforts such as planting trees balance trade-offs between carbon, biodiversity and overall ecosystem function.

* Corresponding author at: Terrestrial Ecology Section, Norwegian Institute for Nature Research - NINA, 0349 Oslo, Norway.
E-mail address: zander.venter@nina.no (Z.S. Venter).

https://doi.org/10.1016/j.scitotenv.2021.145384

1. Introduction

Soil organic carbon (SOC) content is one of the most important properties of soil in determining the characteristics of vegetation that can grow on that soil. In turn, the vegetation characteristics are strong determinants of the amount and vertical distribution (Jobbágy and Jackson, 2000) and forms of SOC in the soil (Baily et al., 2019). Anthropogenic interference in this feedback through modification of the vegetation characteristics (e.g. clearing natural vegetation) and also by manipulation of the soil (e.g. ploughing, fertilizing) has resulted in large-scale changes to SOC globally. For example, land use change resulting from cropping and grazing over the last 12,000 years has led to an estimated 116 Pg C loss in the top 2 m of soil with most of this occurring in grasslands, savannas and croplands (22, 22, 21 Pg C respectively; Sanderman et al., 2017). Sanderman et al. (2017) estimate that while some areas gained soil C from cropping, the median loss globally is 26%. SOC is also of global importance because the size of the SOC pool (1500 Pg C) is ca. three-fold that of above-ground vegetation (450 Pg C; Friedlingstein et al., 2020). Since anthropogenic manipulation can change the SOC pool dramatically, the large SOC pool has been the focus of decades of discussion and many initiatives (e.g. Lal, 2004) to explore and enhance its potential to sequester atmospheric CO_2. Despite this focus, 87% of global carbon stocks are actually oceanic (ca. 38,000 Pg C, mostly inorganic) with 11% being terrestrial (4655 Pg C) and 2% in the atmosphere (860 Pg C) (Friedlingstein et al., 2019; Le Quéré et al., 2018). Furthermore terrestrial coal, gas, oil (5000–10,000 Pg C; Houghton, 2007) as well as permafrost (Friedlingstein et al., 2020) make up two-thirds of land C stocks. It is therefore not the dominant size of the SOC pool (despite frequent claims to the contrary), that has resulted in the focus of attention on its capacity to sequester C, but the fact that manipulation of the SOC pool is perceived as being feasible.

Manipulation of SOC is seen as part of natural climate solutions or efforts to increase carbon storage by restoration, conservation or improved management of native and agricultural systems so that global warming is stabilized below the 2 °C level (Goldstein et al., 2020; Griscom et al., 2017). Some initiatives to sequester C have been criticised for inaccurate estimates and predictions of SOC among other challenges (Rumpel et al., 2020). Thus in order to understand the potential of soil to support vegetation and also to sequester C, quantification of the potential SOC is required. This may be achieved by examining the SOC in sites that have been only indirectly impacted by humans and understanding its drivers. Apart from the direct importance of SOC, it is also a useful proxy for measure of soil health (Mills and Fey, 2004) because it tends to correlate positively with soil properties such as infiltrability, aggregate stability, erodibility, water-holding capacity, nutrient-holding capacity, microbial biomass, soil respiration and availability of plant nutrients. Thus accurate assessments of SOC and the way in which it is changing are vital.

The amount of SOC is strongly determined by the input of C and longevity of C in the soil and consequently depends on the balance between net primary productivity and decomposition and other processes that promote SOC loss/retention (e.g. fire and grazing). This balance is determined by climatic factors and elevation at global and regional scales, while soil texture, mineralogy, and topography that vary at smaller scales interact with climate to determine SOC locally (Houghton, 2007; Huang et al., 2018). For example, in the cold wet climates of northern latitudes, primary productivity exceeds decomposition because photosynthetic rates are not limited by moisture, but microbial mineralization is limited by cold, resulting in accumulation and high SOC (Houghton, 2007). Generally, arid regions have low SOC due to low primary production, while the tropics often have intermediate SOC levels due to high rates of primary productivity compensating for rapid decomposition. Temperate ecosystems may have seasonally high primary productivity and seasonally low decomposition rates resulting in an accumulation of SOC (Huang et al., 2018). Legacy climate is also a major determinant of SOC. For example, an arid grassland may have relatively high SOC concentrations if it was previously forested (Delgado-Baquerizo et al., 2017). Parent material and soil characteristics are particularly important determinants of SOC stabilization, which is dependent on mineral association and aggregate formation (Kleber et al., 2011) with the exception of pyrogenic and fossil C (Marschner et al., 2008).

Climate change is likely to have important consequences for SOC due to alteration of the inputs from vegetation, decomposition related processes and fire regimes. Because decomposition is a temperature- and moisture-sensitive process (Knorr et al., 2005), elevated temperature has the potential to increase the flux of CO_2 from soils. For example, models with constant inputs estimated 11–16% increased loss of SOC in central Europe (Wiesmeier et al., 2016). Changes in vegetation due to climate change and elevated CO_2 are also likely to influence SOC but due to the complex interactions between inputs and losses of SOC it is difficult to predict what the net outcome will be (McGuire et al., 1995; Zhou et al., 2019). Global climate induced increases in extreme fire weather conditions resulting in a 22% increase in burned area (Abatzoglou et al., 2019) also contribute to changes in SOC both directly through formation of pyrogenic C and by influencing vegetation. While these climate-linked changes are undeniably important over vast areas, land use changes can yield even greater positive and negative effects on SOC (Houghton, 2007; Zhou et al., 2019).

Globally, the levels of SOC are highest at high latitudes where low temperature slows decomposition and where there is currently still a net sink for CO_2 (Houghton, 2007). This raises the question of whether sequestration in temperate ecosystems, such as in South Africa (SA), can be meaningful for global CO_2 sequestration? The argument has been made that despite relatively low SOC percentages, extensive areas can contribute to a high potential for sequestration. South Africa is thought to have lost 2 Pg C (going from 15.8 to 13.8 Pg C) since 10,000 BCE, largely due to grazing, the main land use (Griscom et al., 2017). While global loss estimates due to cropping are larger per unit area, total losses from grazing are more than cropping due to its spatial extent, e.g. 33 vs. 31% losses (Sanderman et al., 2017). Grasslands of southern Africa, Argentina and Australia are hotspots of SOC loss and could be targeted for restoration efforts (Sanderman et al., 2017). Despite this, herbivory is a natural part of African ecosystems (Venter et al., 2017). Fires are another important driver of plant biomass production in African grassland and savanna ecosystems (Archibald et al., 2005). While frequent fires decrease soil C and N concentrations (−13%), moderate burning increases them (+19% C and +18% N) in savannas and grasslands (Pellegrini et al., 2018). Pyrogenic soil C (PyrC; Jones et al., 2019) represents 14–60% of total soil organic C (Jones et al., 2019; Reisser et al., 2016). PyrC or charcoal is resistant to microbial degradation and stable on timescales relevant to anthropogenic climate change and its potential mitigation, i.e. centuries to millennia (Jones et al., 2019). In SA, the Grassland, Savanna and Fynbos biomes are all fire-driven or -prone, unlike the Karoo, Thicket and Forest biomes (Mucina et al., 2018). Fire is an important driver of nutrient cycling in these fire-prone ecosystems and similar ones globally. Fire and herbivory are also important in maintaining productivity in native grasslands by reducing woody plant encroachment, which, for example, has increased by 8% in sub-Saharan Africa over the last three decades (Venter et al., 2018).

With the advent of cloud-based computing and satellite remote sensing, our ability to create wall-to-wall maps of SOC has advanced significantly in recent years (Xiao et al., 2019). The standard approach adopted by the UNCCD includes assigning SOC densities to land cover/use categories and then extrapolating over space using coarse-resolution global land cover products (Mattina et al., 2018). Changes in land cover are then used to infer national changes when reporting on carbon trends to the UNCCD. More advanced geostatistical approaches such as spatial or regression kriging rely heavily on soil sampling data to interpolate SOC surfaces, often informed by a relationship to basic edaphic variables like elevation (Lamichhane et al., 2019). Two

such approaches have been used to map soil carbon over SA at 1 km resolution (Department of Environmental Affairs, 2015) and aggregated to terrain units (Schulze and Schütte, 2020). One disadvantage of these approaches is that, unless new soil samples are collected, they do not permit monitoring of SOC change. Developments in the field of machine learning and remote sensing have advanced soil mapping science (Padarian et al., 2020; Stockmann et al., 2015) to the point where it is possible to tentatively map SOC in space and time (Heuvelink et al., 2020). Such advances have led to a proliferation of national-scale (e.g. Brazil: Gomes et al., 2019; United States: Guevara et al., 2020; Madagascar: Ramifehiarivo et al., 2017) and global-scale (Hengl et al., 2017) soil carbon maps. However, global maps of SOC may be locally biased and inaccurate, particularly where the global model used to infer SOC did not have access to national or provincial soil reference data (Cramer et al., 2019a, 2019b). Further, national-scale maps in SA to date have been limited in spatial resolution to 1 km. These limitations preclude the ability to detect and monitor SOC dynamics at spatial scales that are relevant to land managers (e.g. conservationists and farmers).

Considering the importance of SOC in ecosystem functioning and agriculture and initiatives to sequester C in SOC, it is important to know what the potential SOC content of temperate systems is. This may provide a benchmark to target for restoration of SOC in transformed landscapes. Furthermore, understanding the likely SOC trajectories over the country and at landscape scales will allow for further analysis of the drivers of SOC change. Firstly, we aimed to build upon previous SOC mapping efforts in SA to create a national long-term average SOC map of greater accuracy and spatial resolution than its predecessors. Secondly, we aim to advance the methodological state-of-the art in digital soil mapping by incorporating Landsat satellite imagery in a machine learning workflow to map decadal SOC changes at 30 m spatial resolution and national extent. Comparison with other contemporary (regional) models is also informative in identifying bottlenecks to the modelling enterprise. Finally, using the trend maps we test the hypothesis that, given the recent encroachment of woody plant cover into savannas, changes in national fire regimes and global warming trends, there has been a net sequestration of carbon in soils within natural areas of SA. The accurate and high-resolution maps of mean SOC and SOC trends presented here will inform future enquiry into the drivers of SOC change as well as the potential of areas to increase SOC given their inherent climate and edaphic limitations. This understanding will help us access the potential to increase soil C storage while maintaining ecosystems integrity.

2. Methods

2.1. Study area

South Africa (SA) comprises 9 biomes (Fig. 1; desert and coastal biomes are not shown) where there is a distinct East-West aridity and productivity gradient. The Succulent Karoo in the West is arid with a low austral winter rainfall (ca. 100–200 mm) and relatively low productivity and SOC soils while the Grassland and Savanna biomes in the East receive rain in the austral summer (ca. 800 to >1500 mm) and include relatively higher productivity and SOC (Department of Environmental Affairs, 2015; Hijmans et al., 2005). Only 16% of SA is considered arable and the dominant land use is livestock and wildlife farming on native rangelands (79% of SA; Statistics South Africa, 2020), notably in the Karoo biomes, Grassland and Savanna biomes. The Fynbos, Grassland and Savanna biomes evolved with and are dependent on fire for nutrient cycling (Mucina et al., 2018). Dominant soils are Arenosols (sandy soils low in organic matter), Regosols (mineral soils) as well as more fertile Luvisols and Cambisols as classified by the World Reference Base for Soil Resources (IUSS Working Group WRB, 2015). High SOC soils in SA largely overlap with Acrisols and Regosols (Agriculture Organization of the United Nations. Land and Water Development Division, 1993). Locally, the predominant soils are classified as lithic and oxidic (sandy or rocky low fertility soils) while soils that are cumulic (e.g. of aeolian, colluvial and alluvial origins) are also widespread but organic soils cover very little of the country soil (Fey, 2010; Soil Classification Working Group, 1991). The high SOC Acrisols and Regosols of the WRB roughly overlap with 'humic' soils in the local classification and are concentrated in the relatively moist eastern side of SA. Generally, much of SA comprises old, climatically buffered infertile landscapes (OCBILS; Hopper et al., 2016; Hopper and Lambers, 2009). These OCBILS are globally associated with 12 of the 35 global biodiversity hotspots, of which 3 occur in SA.

2.2. SOC sampling data

Survey data on soil profiles and topsoil cores were collated from four data sources. These included a national soil profile database from the Agricultural Research Council of South Africa, a regional subset of the global soils database collated by the International Soil Reference and Information Centre (ISRIC), and two research-based private collections; one maintained by Heidi Hawkins and the other by the Gamtoos Irrigation Board and the Department of Environmental Affairs (GIB & DEA Fig. 1). Soil samples were collected under different sampling designs (summarised in Table S1). Soil organic carbon was analysed using the Walkley-Black oxidation method (Walkley and Black, 1934) or dry oxidation after removal of carbonates, where correlation between SOC using these methods is high (r^2 of 0.96; Dieckow et al., 2007). We filtered the datasets for samples collected in natural areas after 1984 (before which no Landsat satellite data are available). Natural areas were defined by the 20-m resolution 2018 South African National Land-Cover dataset (Thompson, 2018) as any land cover other than water, urban (artificial surfaces), mines or cultivated land (172,000 km^2 or 14% of the country). We chose to exclude these land use types because the drivers of SOC dynamics are distinct from those in soils under natural vegetation. SOC in cultivated soils is influenced by tillage, crop rotation, crop residue management, fertilization, fallow periods and irrigation. We did not have the spatial data to act as proxies for these processes and anticipate that including agricultural land would over-estimate SOC on natural land. The spatial and temporal filter left us with a total of 5834 soil samples (ARC: 5429, ISRIC: 41, Hawkins: 135, GIB & DEA: 229) distributed over 35 years and spread over South Africa (Fig. S2).

We used only topsoil samples from all databases with a recorded depth of between 0 and 20 or 30 cm. SOC stock values for each sample were calculated using the following formula:

$$SOC_{stock}\ (kg\ C\ m^{-2}) = SOC_{concentration}\left(g\ kg^{-1}\right) \times BD\ (g\ cm^{-3}) \times (1-CRF) \times d\ (cm)$$

where *BD* is the bulk density of the soil, *CRF* the proportion of coarse fragments, and *d* is the depth. Where *BD* and *CRF* were not reported in the soil survey databases, we used the betaSoilGrids2019 data (de Sousa et al., 2020) to infer values at given sampling locations. We acknowledge that this inherits the uncertainty in the BD dataset, however these are mostly low with only western coastal and some Fynbos mountainous areas having medium uncertainty (soilsgrid.org). In addition, we could not source a more reliable alternative.

2.3. Environmental covariates

Environmental covariates were collected as model inputs to help explain both the spatial and temporal variation in SOC over SA. All data were processed within the Google Earth Engine cloud computing platform for geospatial analysis (Gorelick et al., 2017). Covariates were collected as proxies or indicators of climatic, biological and morphometric determinants of SOC formation (Table 1) in line with soil mapping best practice guidelines (Hengl and MacMillan, 2019). These included static covariates (long-term averages that do not change over time) and

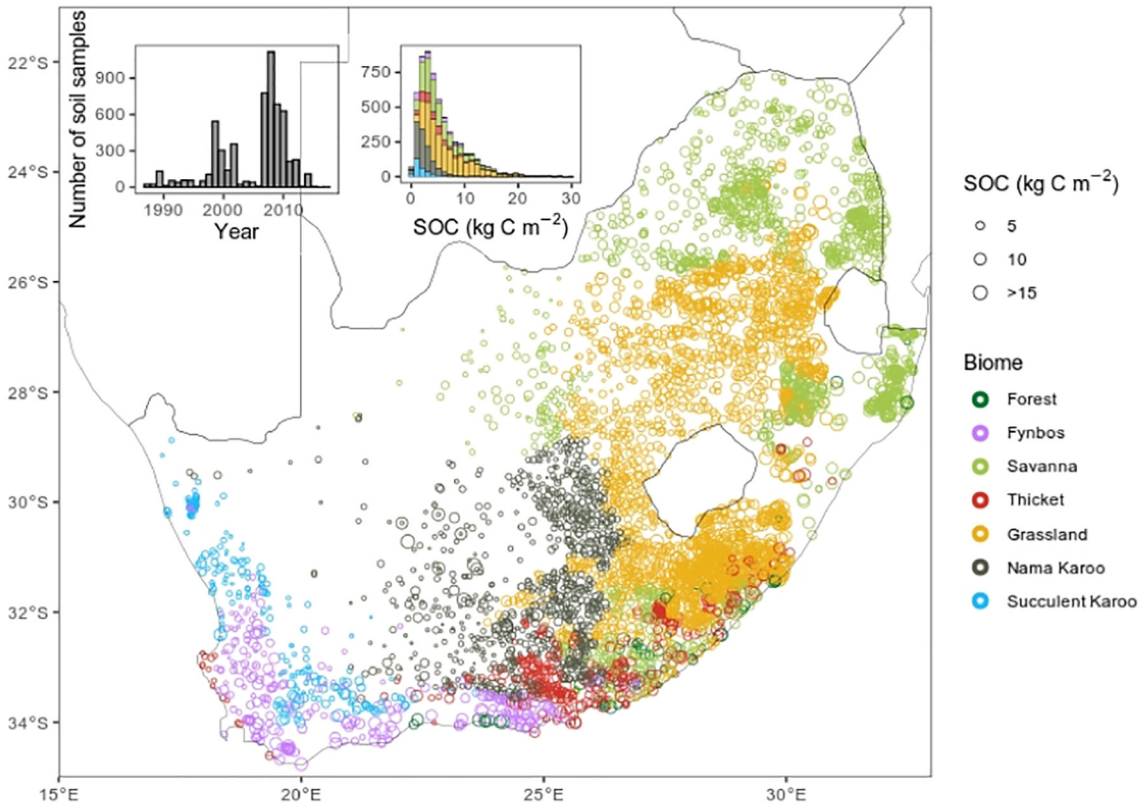

Fig. 1. Distribution of soil sample locations over South Africa. Sample locations are coloured by the biome in which they occur and sized based on the observed SOC value. Inset graphs show the distribution of samples over time and the distribution of SOC values per biome.

dynamic covariates (covariates that change with time), which have global coverage and thereby promote the transferability of these methods.

The primary static covariates describing biological processes included the long-term (1984–2019) mean of leaf area index (LAI) and fraction of photosynthetically active radiation (FAPAR) derived from the Advanced Very High Resolution Radiometer (AVHRR) satellite provided by the National Oceanic and Atmospheric Administration (Claverie and Vermote, 2014). We calculated average net primary productivity and fire frequency at 500 m resolution between 2000 and 2019 using datasets ("MOD17A3HGF V6" and "MCD64A1") derived from the Moderate Resolution Imaging Spectroradiometer (MODIS). Along with fire, herbivory is also an important driver of biogeochemical cycles (Venter et al., 2017) and therefore, we included gridded livestock densities (Robinson et al., 2014) as a covariate. We also included data on the frequency of bare surfaces (Dematté et al., 2020) and mean fractional woody plant cover (Venter et al., 2018) based on methods using the Landsat satellite archive. Static covariates describing morphometric processes included terrain variables listed in Table 1 and derived from the digital elevation model produced with the Shuttle Radar Topography Mission (Farr and Kobrick, 2000). These data also included ecologically-relevant indices describing landforms and physiographic diversity of terrain including the topographic diversity and position indices and the continuous heat-insolation load index (Theobald et al., 2015). The final group of static variables characterizes climatic processes and was derived from the WorldClim V1 Bioclim dataset (Hijmans et al., 2005).

Dynamic covariates were derived from the spectral reflectance data collected by the Landsat 5, 7 and 8 satellites at 30 m spatial resolution between 1984 and 2019. The imagery provided in Google Earth Engine has been orthorectified and atmospherically corrected to produce surface reflectance products. We masked clouds, cloud shadow and snow using the 'pixel_qa' band. Due to slight differences between sensors aboard Landsat satellites (Holden and Woodcock, 2016), cross-calibration of reflectance values is important when implementing time series analysis (Zhu, 2017). We applied published cross-calibration coefficients to harmonise Landsat 8 reflectance values with the other Landsat collections (Roy et al., 2016). Annual median composite images were calculated for all bands including the normalized difference vegetation index (NDVI), which has been widely used as a proxy for vegetation productivity and cover (Pettorelli et al., 2005; Tucker, 1979) and is therefore expected to correlate to SOC. We also calculated the 10th and 90th percentile NDVI composites for each year in an attempt to characterize vegetation phenologies (e.g. annual grasses versus perennial woody plants), which might be an important determinant of SOC (Table 1). For each soil sample, we extracted the year-specific satellite composite values for the 30 × 30 m pixel intersecting the soil sample location. Therefore, the Landsat-derived covariates are dynamic data that vary temporally with the date of soil sample collection.

2.4. SOC modelling

To map SOC over space and time, we used a machine learning workflow leveraging the Random Forest (RF) regression tree model (Breiman, 2001). RF is one of the most commonly used models in digital soil mapping (Khaledian and Miller, 2020; Padarian et al., 2020) due to its ability to handle nonlinear interactions between covariates and skewed response data like SOC. To avoid overfitting and aid model interpretability, we eliminated unnecessary and collinear covariates with a two-step process. First we performed recursive feature elimination (RFE) which is a process akin to backward regression (Guyon et al., 2002). RFE produces a model with the maximum number of covariates and iteratively removes the weaker explanatory variables until a specified number of covariates is reached. Secondly, we screened

Table 1
Environmental covariates used to model SOC over South Africa.

Type	Process category	Spatial resolution (m)	Variable
Static	Biological	5000	FAPAR mean
			FAPAR standard deviation
			LAI mean
			LAI standard deviation
		500	Fire frequency
			Livestock density
			Net primary productivity
		30	Bare surface frequency
			Fractional woody cover
	Morphometric		Elevation
			Terrain aspect
			Terrain slope
			Topographic diversity index
			Topographic position index
			Continuous heat insolation load index
	Climatic	1000	Mean annual precipitation
			Mean annual temperature
			Precipitation coldest quarter
			Precipitation driest month
			Precipitation driest quarter
			Precipitation seasonality
			Precipitation warmest month
			Precipitation warmest quarter
			Precipitation wettest quarter
			Temperature annual range
			Temperature coldest quarter
			Temperature diurnal range
			Temperature driest quarter
			Temperature seasonality
			Temperature warmest quarter
			Temperature wettest quarter
Dynamic	Biological	30	Blue band reflectance
			Green band reflectance
			Red band reflectance
			Near infrared band reflectance
			Short-wave infrared reflectance 1
			Short-wave infrared reflectance 2
			NDVI 10th percentile
			NDVI 50th percentile
			NDVI 90th percentile

Abbreviations: FAPAR - fraction of photosynthetically active radiation; LAI - leaf area index; NDVI - normalized difference vegetation index.

for multicollinearity in the covariate set by calculating variance inflation factor (VIF) values for each covariate and only including those with a VIF of less than 5 (Zuur et al., 2010). The excluded collinear variables are listed in supplementary Fig. S2. The RF models were run with hyperparameters *ntree* set to 500 and *mtry* set to the square root of the number of covariates.

To evaluate the uncertainty associated with the RF predictions, we used external validation by withholding 30% of the dataset from the model training stage and thereafter tested model predictions against it. According to best practice (Piñeiro et al., 2008), we regressed observed SOC on predicted SOC to derive the root mean square error (RMSE), mean absolute error (MAE) and adjusted R^2 as measures of model accuracy and fit (Willmott, 1981). We repeated this process 100 times in a bootstrapping procedure with different randomly selected training and testing sets each time. The mean of the resulting RMSE and R^2 values were then calculated as well as the mean error per soil sampling location to give an indication of how model error varies over space. The RF algorithm also measures the relative importance of each covariate by quantifying the increase in prediction errors when a predictor is permuted in the validation data. These importance scores were averaged per covariate in order to understand what is driving the model predictions.

2.5. SOC trend calculation

The trained RF model was then used to make wall-to-wall predictions of SOC at 30 m resolution over SA for each year between 1984 and 2019. We were able to do this because the model was trained on satellite data synced to the year of soil sample collection for each soil survey site. We used the annual Landsat composites to predict annual SOC values for each pixel. Long-term average SOC was calculated as the mean value across all annual predictions. The magnitude of the trend in SOC was calculated for each 30 × 30 m pixel using the Sen's slope (Sen, 1968) estimator across all annual SOC prediction maps. The Sen's slope differs from simple linear regression in that it is a non-parametric regression that is robust against outliers and skewed data (Wilcox, 2010). The relativized change in SOC was calculated as:

$$\Delta SOC\ (\%) = m \div SOC_{mean} \times 100$$

where m is the Sen's slope and SOC_{mean} is the long-term mean for the pixel in question. Due to a lack of repeated measures SOC sampling data (i.e. SOC samples repeated at the same location over time), we could not validate our SOC change predictions.

2.6. Comparison with other SOC products

To compare our SOC predictions with previous mapping efforts, we extracted SOC values for all sampling locations from the betaSoilGrids2019 dataset (Hengl et al., 2017; SoilGrids, 2019) at 250 m resolution, the African iSDA soils dataset at 30 m resolution (currently under review; Hengl et al., 2020), the SA national terrestrial carbon sinks assessment (Department of Environmental Affairs, 2015) at 1000 m resolution, and a recently produced national terrain-unit based SOC map (Schulze and Schütte, 2020) rasterized at 100 m resolution. The Schulze and Schütte (2020) dataset reports percentage soil organic carbon and was converted to SOC with bulk density and coarse fragments from SoilGrids. As with our RF uncertainty assessment, we regressed predicted SOC on observed SOC and calculated RMSE, MAE and R^2 for each data product.

Table 2
Summary statistics on long-term soil organic carbon (SOC) stocks, density and change per biome in South Africa. Values in square parentheses are 5th and 95 percentile values.

Biome	Area natural land (km^2)	SOC stock (Pg C)	SOC density (kg C m^{-2})	Net SOC change (%)	Net SOC change (kg C m^{-2})
Forest	6775	0.07	9.9 [6; 13]	0.8 [−2.6; 5.7]	0.08
Fynbos	63,944	0.4	6.0 [2.4; 9]	0.5 [−5.1; 7.3]	0.03
Grassland	269,920	2.02	7.1 [3; 12]	1.7 [−3.9; 8.7]	0.12
Nama Karoo	314,638	0.73	2.3 [1; 4.3]	−0.6 [−7.5; 6.2]	−0.01
Savanna	404,757	1.9	4.8 [1.6; 10]	−0.3 [−10; 9.2]	−0.01
Succulent Karoo	86,230	0.2	2.4 [1.4; 4.6]	−0.4 [−5.7; 4.8]	−0.01
Thicket	38,306	0.27	7.0 [2.5; 11.9]	0.7 [−4.7; 7]	0.05
Total:	1,184,571	5.59	5.6	0.3	0.02

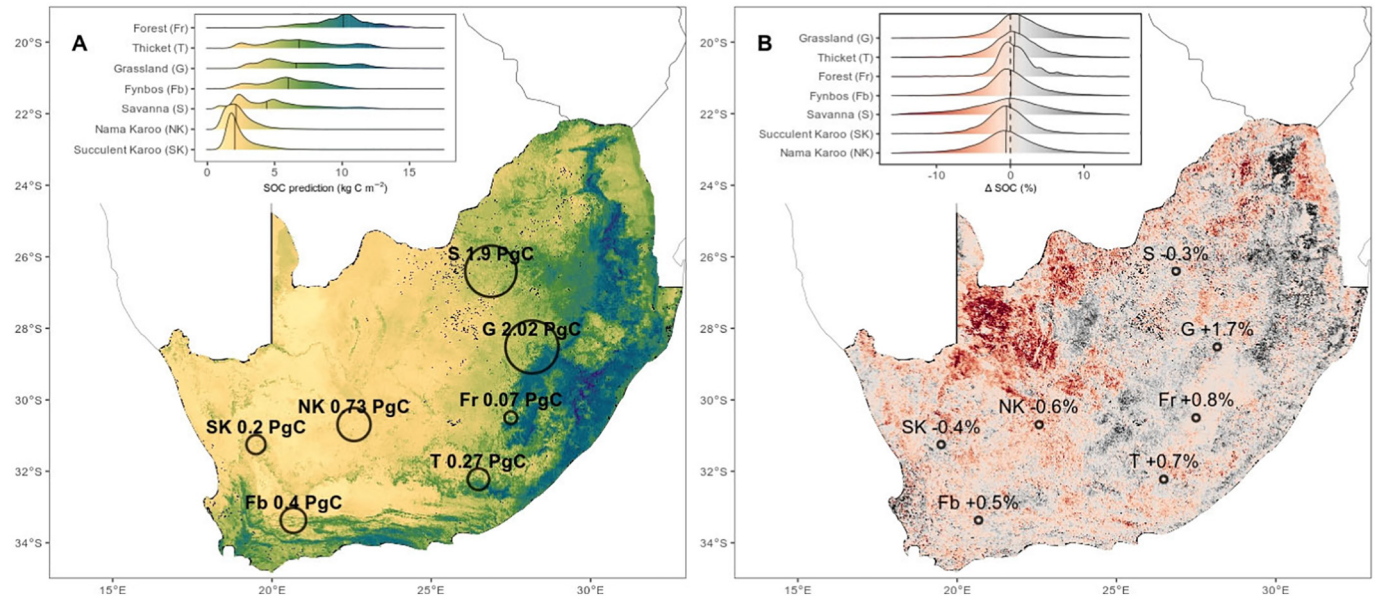

Fig. 2. Predicted long-term average SOC (A) and changes (B) between 1984 and 2019. Change is expressed as a percentage of the long-term average for each pixel. Inset plots in A and B show the density distribution of data values for each biome. White circles and text on the map in A indicate total SOC amounts within each biome in petagrams (10^{12} kg). Black text on the map in B indicates biome average changes in percent.

3. Results

3.1. SOC spatio-temporal predictions

We estimate a total topsoil SOC stock of 5.6 Pg C in natural areas with a median SOC density of 6 kg C m^{-2} (IQR: interquartile range 2.8 kg C m^{-2}) or 60 t ha^{-1} (Table 2; Fig. 2). The regional distribution of SOC tends to follow the East-West aridity gradient, with greatest stocks in the mesic Grassland and Savanna biomes, and smallest stocks in the Karoo biomes in the West (Table 2). The Grassland biome has the second highest SOC density and therefore, although it covers half the area of the Savanna, it amounts to a greater fraction of the national SOC stock. In contrast, the forest biome contains the highest average SOC densities, yet due to its limited distribution accounts for the smallest fraction of the national SOC stock.

Over 35 years, SOC underwent a net increase of 0.3% (relative to long-term mean) with the greatest net increases (1.7%) and decreases (−0.6%) occurring in the Grassland and Nama Karoo biomes, respectively (Table 2). SOC trends were very heterogeneous over space, with areas of large SOC loss and sequestration within close proximity (Fig. 2). Although the net changes reported at the biome level (Table 2) were relatively small, large trends (sequestration and loss of up to 25% of long-term mean) were evident at provincial and landscape scales. These heterogeneities reveal fence-line contrasts in SOC dynamics, presumably driven by grazing, browsing or frequent burning (Fig. 3A and B), and woody plant clearing/harvesting (Fig. 3C and D).

3.2. Model performance and uncertainty

The annual standard deviation in LAI was the most important variable in the RF model, followed by mean annual precipitation and elevation above sea level (Fig. 4). These highlight the importance of climatic and morphometric constraints on regional variation in SOC. We found four dynamic (satellite-derived) variables within the 15 most important covariates explaining the spatio-temporal variance in SOC (Fig. 4). Among these, two measures of vegetation greenness (NDVI 90th and 10th percentile) were present, highlighting the importance of vegetation cover as a proxy for SOC.

Our final RF model produced a mean absolute error of 1.6 kg C m^{-2} (Figs. 5 and 6A). Model uncertainty was not evenly distributed over space, with the highest median accuracies within the Grassland and Savanna biomes (Fig. 5). The model tended to under-predict SOC in arid biomes such as the Succulent Karoo and over-predict in mesic biomes such as the Forest (Fig. 5).

3.3. External comparison

Our SOC mapping approach exhibited lower uncertainty compared to previous national-scale (Fig. 6B and C) and international SOC maps (Fig. 6D). In comparison to the other SOC maps in concert, our map had lower error ($RMSE$ = 2.5 vs 3.6 kg C m^{-2}), greater model fit (R^2 = 0.64 vs 0.27), and less bias. The SoilGrids dataset displayed large negative biases above approx. 5 kg C m^{-2}. In contrast, the two national-scale products exhibited positive biases, over-estimating SOC across the whole range of observed SOC values (Fig. 6B and C). The newly-released iSDA dataset performed better than the other data products, however, it was less accurate relative to our map and underestimated SOC (Figs. 6E and 7E). Apart from modelling accuracies, the advantages of higher spatial resolution are clear when comparing different SOC map products at landscape scales (Fig. 7). The lower spatial resolution (250–1000 m) of previous mapping products obscure landscape variations in SOC that are clearly visible at 30-m resolution.

4. Discussion

The SOC map presented here is at higher resolution, lower uncertainty and exhibits less bias compared to previous lower-resolution (250–1000 m) national SOC mapping efforts. The level of uncertainty associated with our SOC map ($RMSE$ = 2.5 kg C m^{-2}) is comparable to that of other national-scale studies in Argentina ($RMSE$ = 2.04 kg C m^{-2}; Heuvelink et al., 2020) and Madagascar ($RMSE$ = 2.6 kg C m^{-2}; Ramifehiarivo et al., 2017). The 30-m resolution allows

Fig. 3. Landscape-scale predictions of SOC change between 1984 and 2019 for four selected locations in South Africa. Examples of wildlife-livestock fence-line contrasts are shown in the Savanna biome in A, grazing contrasts in the Thicket biomes in B, and examples of presumed woody plant clearing activity in the Savanna-Thicket ecotone are shown in C and D. Very high-resolution satellite imagery are shown for reference and were not used in the SOC model. Image sources: Google, DigitalGlobe.

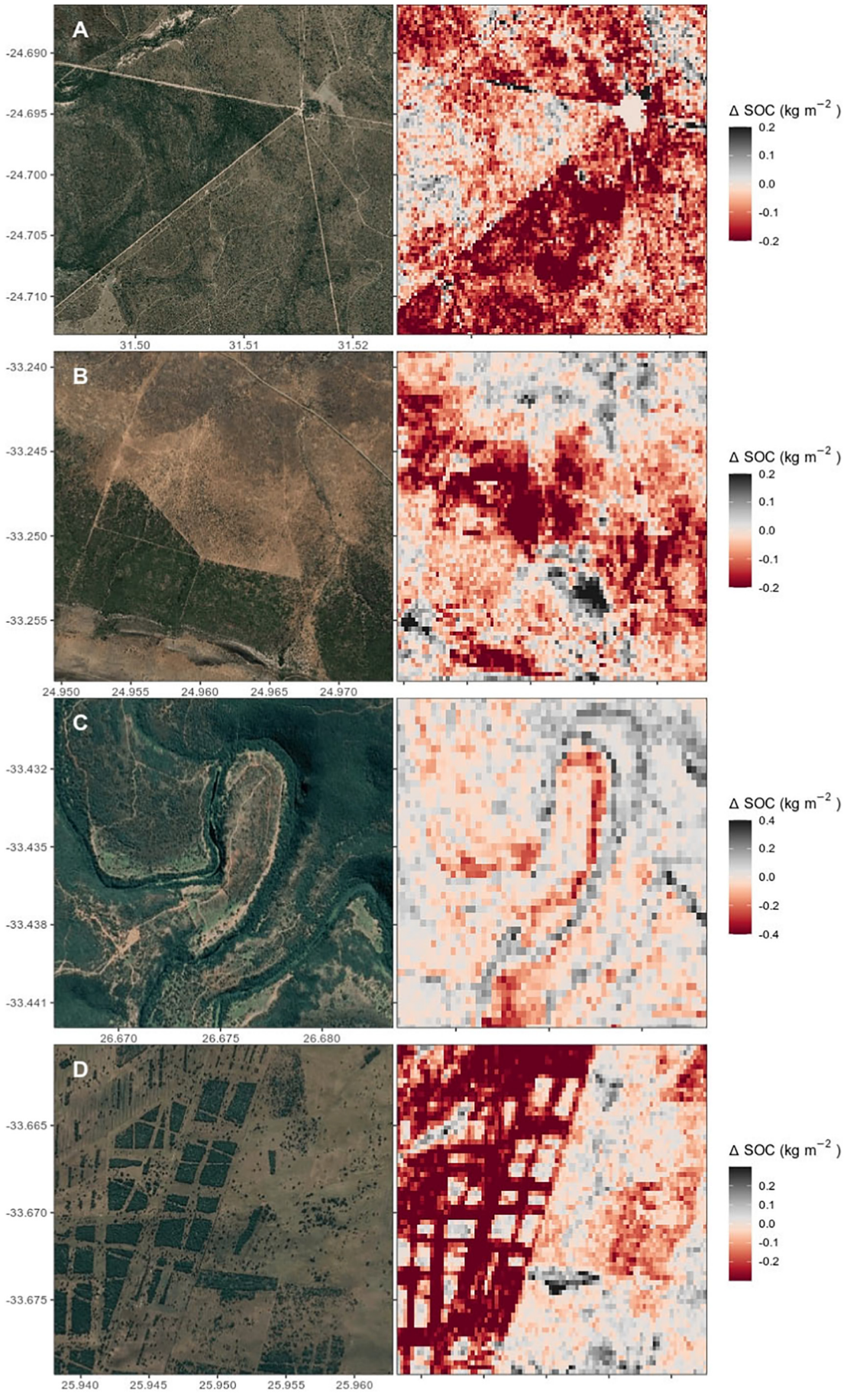
A
-24.690
-24.695
-24.700
-24.705
-24.710
31.50
31.51
31.52
Δ SOC (kg m^{-2})
0.2
0.1
0.0
-0.1
-0.2
B
-33.240
-33.245
-33.250
-33.255
24.950
24.955
24.960
24.965
24.970
Δ SOC (kg m^{-2})
0.2
0.1
0.0
-0.1
-0.2
C
-33.432
-33.435
-33.438
-33.441
26.670
26.675
26.680
Δ SOC (kg m^{-2})
0.4
0.2
0.0
-0.2
-0.4
D
-33.665
-33.670
-33.675
25.940
25.945
25.950
25.955
25.960
Δ SOC (kg m^{-2})
0.2
0.1
0.0
-0.1
-0.2

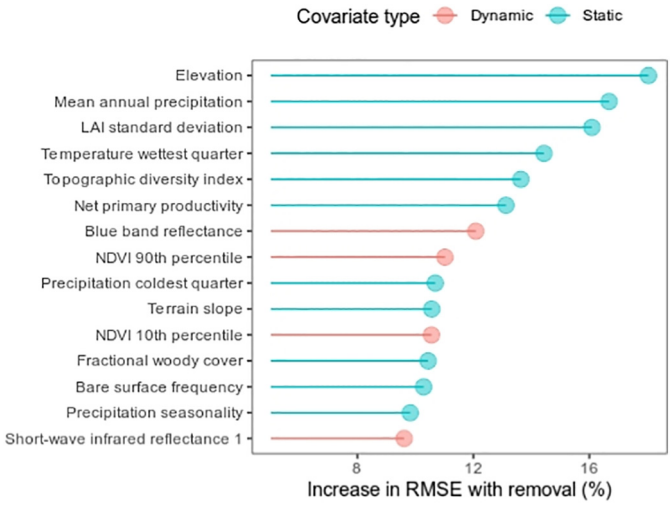

Fig. 4. Variable importance for the final set of covariates used in the Random Forest model to predict SOC over South Africa. Importance is measured as the percentage increase in error if the covariate in question is removed from the model. Dynamic covariates are satellite-derived variables used to monitor changes over time.

for characterization of areas not only at the landscape but also the patch- and farm camp-scale. Apart from the larger number of sample points, the higher resolution satellite data used in our mapping is an important component of the accuracy. Since soils can vary substantially over 10's of metres, using low resolution satellite data (e.g. 1 km) as a correlate with soil characteristics limits the ability of the modelling algorithm to reproduce the variability in soil properties.

Although the SOC temporal change map is based on spatial variation in correlates of SOC, this trend map is perhaps the most interesting and useful aspect of this work since it stimulates further enquiry about drivers of change, while providing land users with a focus for interventions to reverse changes where appropriate, e.g. SOC loss on eroded areas. The mean SOC map indicates important spatial patterns and contrasts at the biome level, suggesting that simple accounting methods for SOC change (e.g., Intergovernmental Panel on Climate Change default emission factors; Eggleston et al., 2006) will misrepresent SOC change in many regions of SA. While biome-scale SOC changes were less than 2%, large SOC trends (sequestration and loss of up to 25% of long-term mean) were evident in some locations, e.g., along fence-lines, that would not be visible at lower resolutions. These landscape and smaller scale differences allow local land use management effects (e.g. animal stocking types and rates, fire regimes) and habitat loss (e.g. woody encroachment from invasive and local plants, erosion) to be visible, questioned and potentially modified. Overall, the regional losses in SOC over the last decades have been relatively small, partially due to the offset resulting from the encroachment of grasslands by woody species.

Comparison between the upper limits of SOC concentrations (Fig. 2) of various biomes is informative about the potential of the individual biomes to sequester carbon. For example, both the Succulent and Nama Karoo regions had relatively low means and upper limits to SOC values compared to the other biomes. These low values are associated with the relative aridity of those systems and indicate that the potential of those systems to sequester C is at best moderate. By contrast, forests have relatively high potential for sequestration, although the spatial extent of forest in SA is rather limited. While it might be naively argued that this requires planting of forests to sequester C in regions that are not forested (e.g. Bonn Challenge, https://afr100.org), the vegetation map of SA indicates the previous extent of vegetation units, independent of

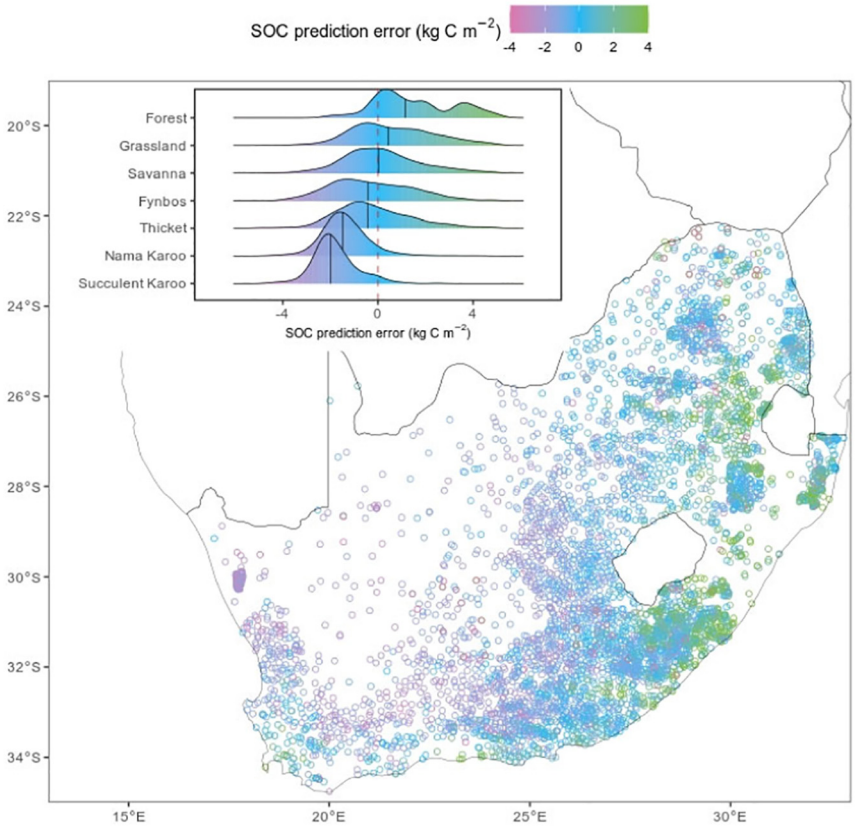

Fig. 5. Spatial distribution of Random Forest model prediction error defined as the residuals from the linear regression of predicted on observed SOC values. Inset graph shows the density distribution of prediction errors per biome.

their current state of transformation. The reason that forests are restricted in extent is because climatic, edaphic or disturbance limitations constrain the extent of closed canopy vegetation. In many cases closed canopy forests occur adjacent to open canopy vegetation across sharp boundaries (tens of metres), indicating edaphic constraints and not anthropogenic modification. A common reason for these sharp boundaries is the difference in fire behaviour in the landscape due to slope breaks, rock scree, drainage lines or wind shadows that results in some areas being more susceptible to fire (Power et al., 2017). Over centuries, these fire patterns have resulted in strong contrasts in soil properties so that currently soil on which neighbouring open canopy vegetation occurs is incapable of supporting closed canopy forest, despite in some cases being derived from the same geology (Cramer et al., 2019a, 2019b). This is in contrast to the incorrect belief that where the climate can potentially support trees, open canopy vegetation represents degraded ecosystems (Bond et al., 2019).

Over the past decade there has been considerable interest in the use of the succulent *Portulacaria afra* (Spekboom), which is an indigenous facultative CAM-photosynthetic plant in SA, to sequester carbon (Mills et al., 2015). This has been based on reported increases in SOC in plantations of Spekboom (Mills and Cowling, 2006). Spekboom-dominated thicket has been used for livestock, especially goat, pastoralism and large areas have been degraded (Lloyd et al., 2002) due to differences in browsing between goats and the indigenous browsers (Lechmere-Oertel et al., 2005; Sigwela et al., 2009). While restoration of prior vegetation should be lauded, attempts to transform other existing vegetation into forest (Bond et al., 2019) or Spekboom-dominated vegetation, motivated by the global carbon market (Mills and Cowling, 2014), are ecologically damaging and prone to failure due to ecological limitations. While some sites may have experienced considerable SOC loss and have great potential for restoration and sequestration, we suggest that in general the potential for sequestration within a biome is relatively fixed by the limits imposed by the biome. Those natural limits are unlikely to change unless the ecosystems are transformed by CO_2- or nutrient-fertilization (e.g. pollution) or management of disturbances such as fire and herbivory. For example, the naturally oligotrophic nature of Fynbos soils has resulted in the vegetation remaining relatively more intact than that of the Renosterveld because Fynbos soils are generally unsuitable for agriculture (Newton and Knight, 2005). However, woody plant encroachment may well represent an example of disturbance that can change SOC.

As part of the trend mapping, we tested the hypothesis that there has been a net sequestration of C across SA given woody plant encroachment trends, declines in burned area and climate warming (Venter et al., 2018). We find a predicted net sequestration of C in soils under natural vegetation where SOC gains were highest in the mesic Grasslands in the east while SOC losses were highest in semi-arid Nama Karoo in the central-west area (Fig. 1). Mesic areas of SA have experienced an increase in woody plant encroachment, i.e. loss of herbaceous habitat (ca. 12% in the Grasslands and Savanna biomes, Venter et al., 2018) and this is likely associated with the observed SOC increase in these areas (we did not find fire frequency to be a driver of SOC in SA). Data from the SA land cover assessments have been used to estimate changes in the spatial extent of the IPCC land cover classes and to generate an estimate of changes in carbon stocks and associated GHG emissions within South Africa's National GHG Inventory (Thompson, 2018). These authors estimate ca. 21,000 Gg CO_2 equivalents have been added to the national C sink through woody plant encroachment (conversion from a grassland to a forest land class). However, if increased SOC is indeed associated with woody plant encroachment, it is in this context a component of ecosystem degradation due to the associated loss of ecosystem function and provisioning services (Archer et al., 2017; Skowno et al., 2017).

The loss of SOC is often associated with ecosystem or land degradation, broadly defined as "the many human-caused processes that drive the decline or loss in biodiversity, ecosystem functions or ecosystem services in any terrestrial and associated aquatic ecosystems" (Scholes et al., 2018). A soil degradation index (SDI) and map of SA, which considers SOC losses as degradation, was developed by Hoffman and Todd (2000). We found that SOC trends over the last 35 years did not (west and central areas) or only partially aligned (mesic east) with the SDI. Areas in our map which showed particularly high rates of SOC loss over the past 35 years were parts of northern Limpopo on the Zimbabwean and Mozambican borders, and Northern Cape between the Namibian border and North West Province. Interestingly, there was no indication that SOC had declined in the subtropical thicket of the Eastern Cape, despite the severe degradation (overgrazing) of this vegetation type over more than a million hectares (Mills et al., 2015), with concomitant losses of large amounts of SOC (Mills et al., 2005). This we suggest is because the degradation of subtropical thicket occurred predominantly during the 1900s and that the degradation is in a stable state, with SOC no longer being lost. Future work would do well to explain the spatial variation in SOC losses and gains at the regional scale in a quantitative manner.

The relative importance of predictor variables in the Random Forest model to predict SOC over SA (Fig. 4) are informative about the conditions that contribute to SOC accumulation. While a number of correlates probably influence SOC through both vegetation productivity and soil carbon decomposition, there are a number of variables that are explicitly related to vegetation density. For example, net primary productivity, NDVI and fractional woody cover all directly relate to vegetation density. Variation in LAI probably relates to the turnover in leaf matter on a seasonal basis. These variables suggest that the limitation on SOC in this region is generally the vegetation inputs. While globally, low temperature strongly facilitates SOC accumulation, within this temperate region it is more likely that water availability and edaphic properties that determine vegetation density are of greater importance. Nevertheless, changes in SOC with elevation may be related to accumulation of SOC under cooler conditions. Future iterations of the map can consider possible drivers of SOC increases such as climate, atmospheric CO_2, fire, woody plant encroachment, and land management, as well as their relative importance in each biome. Understanding drivers of SOC loss and gain in a southern hemisphere country will contribute to a better understanding of SOC dynamics in the global south. In addition, iterations of the map that consider alternative scenarios of restoration and rehabilitations, e.g. restoration of areas that are native but showing signs of erosion, invasive plant invasion, etc. or rehabilitation of agricultural areas to near-native states; and/or alternative cropping to increase C storage (e.g. trees in already transformed areas). These hypothetical scenarios could increase the value of the map as a tool for land use decision making.

Restoration and "natural climate solution" agendas depend on target areas making meaningful contributions to global CO_2 sequestration or reduction in greenhouse gas emissions (Griscom et al., 2017). According to our study the total SOC in SA (5.6 Pg C) is ca. 0.37% of the global terrestrial SOC (1500 Pg C) while SA comprises ca. 0.82% of global land cover. It is estimated that close to 20% of SA's natural land cover is transformed, mainly by cultivation (12%), degradation of the natural cover (5%), urban land use (1%), and forestry (1.5%, Fairbanks et al., 2000). Assuming it is possible to restore ecosystem function to the ca. 5% of degraded native areas (an optimistic assumption), South Africa may be able to contribute 0.23 Pg C to the global C sink, which is only 0.2% of the estimated global SOC loss over the last 12,000 years (Sanderman et al., 2017), in a region which is 0.82% of global land surface.

Our analysis was deliberately limited to soil under natural vegetation. As mentioned, future iterations may expand to include modelling SOC in agricultural soils (Nayak et al., 2019) as well as estimate how much SOC could be gained by restoration of agricultural land and or natural but degraded areas. Such iterations could inform national restoration and rehabilitation efforts by estimating potential additions to the national C stock. Beside C it is important to consider ecosystem functioning as a whole. Three global biodiversity hotspots (Myers et al., 2000) occur in SA and two of these (Cape Floristic Region and Succulent

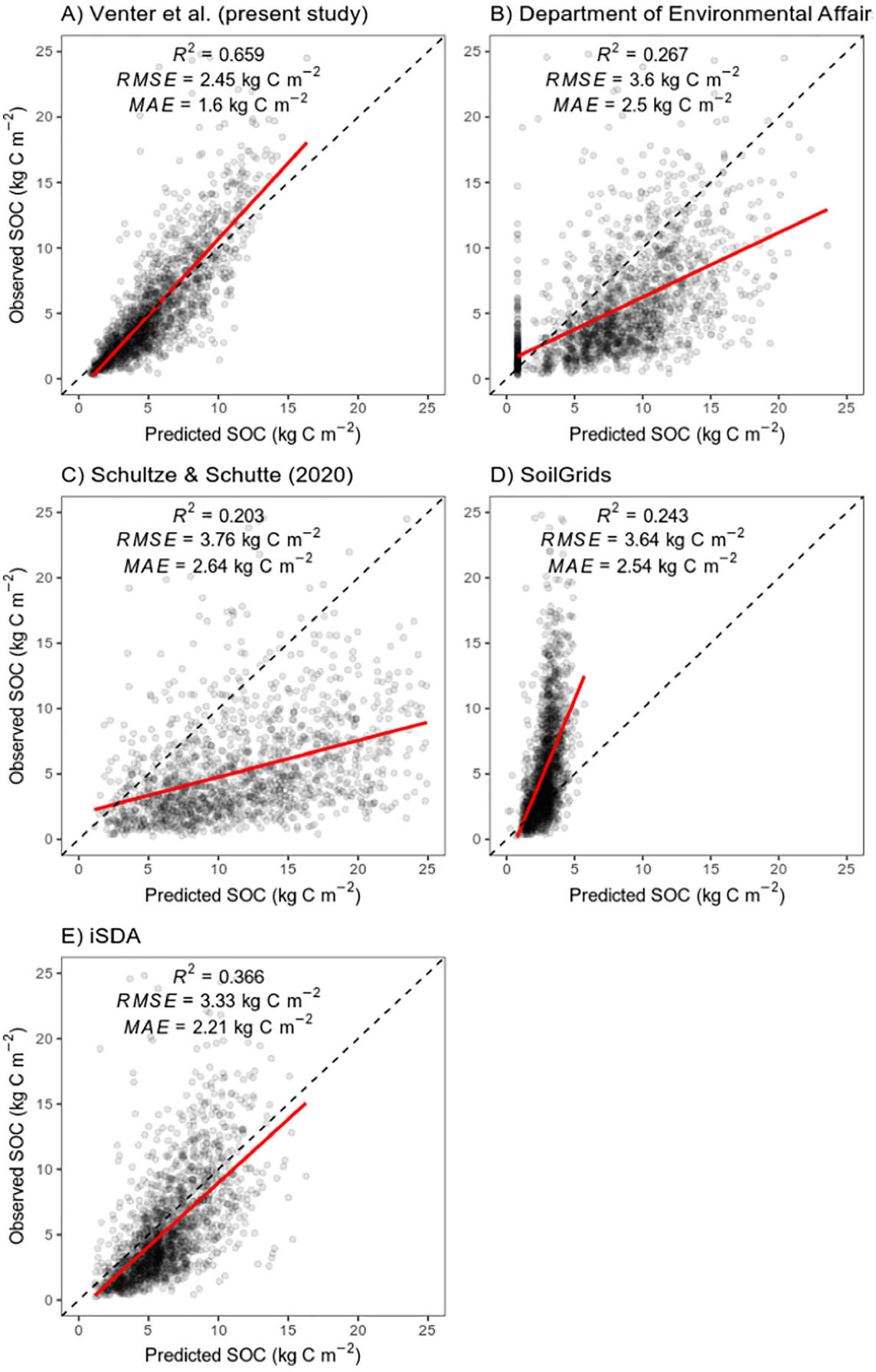
A) Venter et al. (present study)
R^2 = 0.659
RMSE = 2.45 kg C m^{-2}
MAE = 1.6 kg C m^{-2}
B) Department of Environmental Affair
R^2 = 0.267
RMSE = 3.6 kg C m^{-2}
MAE = 2.5 kg C m^{-2}
C) Schultze & Schutte (2020)
R^2 = 0.203
RMSE = 3.76 kg C m^{-2}
MAE = 2.64 kg C m^{-2}
D) SoilGrids
R^2 = 0.243
RMSE = 3.64 kg C m^{-2}
MAE = 2.54 kg C m^{-2}
E) iSDA
R^2 = 0.366
RMSE = 3.33 kg C m^{-2}
MAE = 2.21 kg C m^{-2}
Observed SOC (kg C m^{-2})
Predicted SOC (kg C m^{-2})
0
5
10
15
20
25

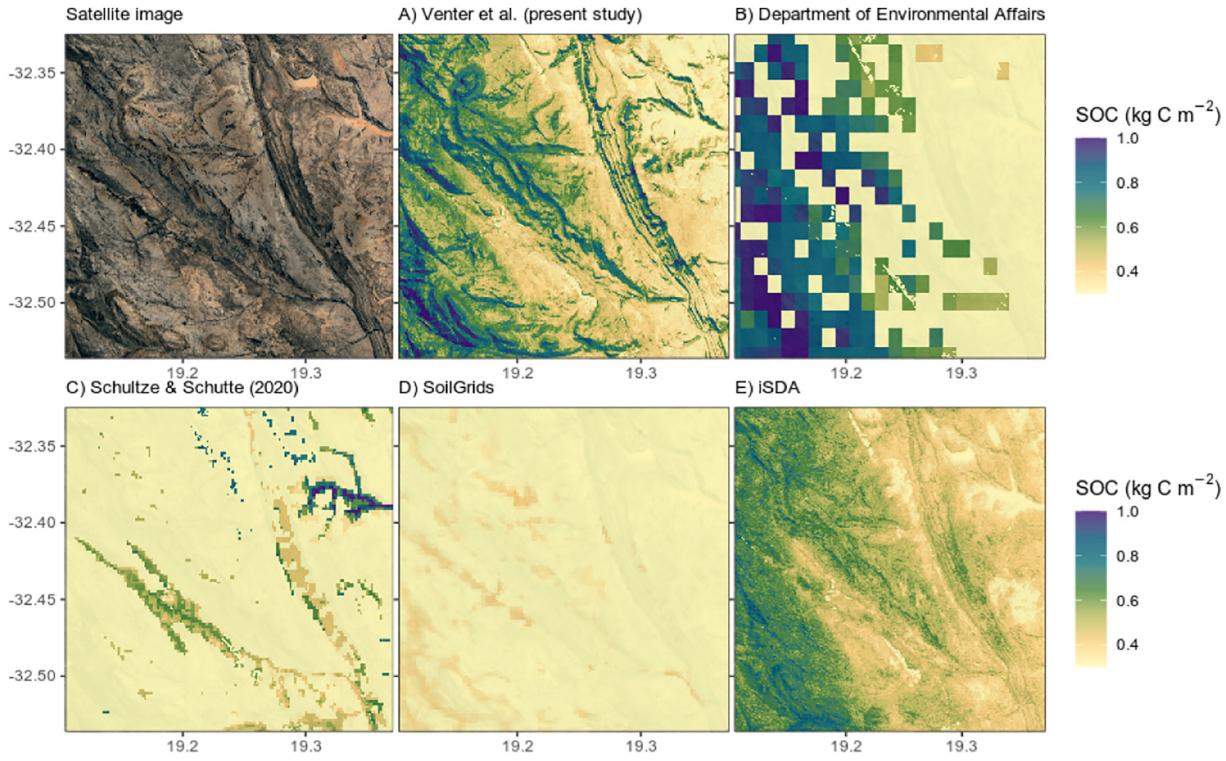

Fig. 7. Landscape-scale maps of long-term average SOC as predicted by the model in the present study (A) and four other data sources (B–E). A very high-resolution satellite image is shown on the top-left for reference.

Karoo) have relatively low SOC and can be considered OCBILS (Hopper et al., 2016; Hopper and Lambers, 2009). Thus low SOC soils can be associated with habitats of high biodiversity and conservation value. Current climate mitigation efforts should therefore balance trade-offs between carbon, biodiversity and overall ecosystem function. Initiatives that trade in C may consider for example vehicles such as Climate, Community and Biodiversity Standards versus those that consider only C, such as Verified Carbon Standards.

Although the SOC map presented here is at unprecedented spatial resolution for a national-scale map, inaccuracies associated with the South African National Land-Cover dataset (Thompson, 2018) and roads are somewhat problematic. Also, the utility of the SOC map for soil carbon policy and management agendas is limited by the map uncertainty ($MAE = 2.6$ kg C m^{-2}). For example, identifying significant differences in SOC, whether at the landscape (e.g. fence-line contrast) or regional (e.g. municipal boundary) scales is limited by this uncertainty, necessitating a difference larger than 5.2 (i.e. 2×2.6) kg C m^{-2}. Aggregation over space does reduce uncertainty because positive and negative errors within a region are cancelled out (Heuvelink et al., 2020). Improved modelling techniques such as progressive machine learning algorithms such as Artificial Neural Networks (Khaledian and Miller, 2020) may also help. The most important antidote to uncertainty is, however, to increase the reference data used to calibrate the SOC model. This aligns with the call for standardized soil sampling and soil monitoring schemes where data, particularly those funded by the state (e.g. governmental research councils), are made open-access for advancing soil science (Smith et al., 2020). International databases of this nature include ISRIC - World Soil Information (https://www.isric.org/) and OpenGeoHub (https://opengeohub.org/about). Collecting repeated measures (i.e. time series) of SOC is particularly important if we are to validate estimates of SOC change such as those mapped in Figs. 2 and 3. In this way, SOC monitoring with remote sensing could follow the model already operationalized in real-time deforestation monitoring (e.g. Global Forest Watch: https://www.globalforestwatch.org/map/).

In summary, the limitations of our SOC maps are that (1) there are uncertainties in the SOC estimation that are difficult to quantify spatially, particularly in the west of the country where there are limited reference data; (2) our estimates of SOC trends have not been validated using repeated soil sampling due to a dearth of such reference data; (3) our data is limited to natural vegetation and the top 30 cm of the soil horizon. Despite these limitations, our maps serve as useful counterpoints to both global (SoilGrids) and continental (iSDA) maps of SOC. Firstly, we use a denser set of reference data in a model specifically calibrated to SA which produces less bias and greater accuracy than the iSDA 30 m map. Secondly, by excluding SOC samples from cultivated lands, we limit the potential for over-estimating SOC under natural vegetation. This is because cultivated lands are generally located on nutrient rich soils and may bias model extrapolation into non-cultivated areas. Finally, by utilizing 35 years of satellite data, we offer novel maps of SOC change which form the basis for further validation and development.

5. Conclusion

The accurate high-resolution map developed here for natural areas in South Africa (84% of the land area) furthers our understanding of how climate, morphometrics and ecosystem processes interact to determine SOC in an area of the world with sparse data availability. This should be useful for identification of areas in need of protection or

Fig. 6. SOC mapping uncertainty based on regression of predicted on observed SOC values for the present SOC model (A) and four other data sources (B–E). Data points represent the validation soil sample data (n = 1808; withheld from model training) with a red linear regression line and dashed 1:1 line for reference.

restoration. We should be cognizant, however, that SOC increases are limited by inherent climate and edaphic characteristics of the areas and that CO_2 mitigation efforts should balance trade-offs between carbon, biodiversity and overall ecosystem function.

Data availability

The long-term SOC mean and trend maps produced in this study are available here: https://zenodo.org/record/4384692#.X-IEC9hKjIU. Predictor variables used in the modelling are available here: https://earthengine.google.com/ Soil survey data are available from here: https://www.isric.org/. The research soil survey data are available from the authors upon request. The Agricultural Research Council needs to be approached independently for their soil survey data.

CRediT authorship contribution statement

ZV, HH, MC, and AM designed research, provided data and wrote the paper. ZV analysed data.

Declaration of competing interest

The authors declare that they have no known competing financial interests or personal relationships that could have appeared to influence the work reported in this paper.

Acknowledgements

We thank the South African Agricultural Research Council for providing data on soil carbon. We thank the National Research Foundation and Patterson Foundation for funding to HJH for soil carbon data collection.

Appendix A. Supplementary data

Supplementary data to this article can be found online at https://doi.org/10.1016/j.scitotenv.2021.145384.

References

Abatzoglou, J.T., Williams, A.P., Barbero, R., 2019. Global emergence of anthropogenic climate change in fire weather indices. Geophys. Res. Lett. 46, 326–336. https://doi.org/10.1029/2018GL080959.

Agriculture Organization of the United Nations. Land, Water Development Division, 1993. Global and National Soils and Terrain Digital Databases (SOTER): Procedures Manual (Food & Agriculture Org).

Archer, S.R., Andersen, E.M., Predick, K.I., Schwinning, S., Steidl, R.J., Woods, S.R., 2017. Woody Plant Encroachment: Causes and Consequences, in: Rangeland Systems. Springer, Cham, pp. 25–84.

Archibald, S., Bond, W.J., Stock, W.D., Fairbanks, D.H.K., 2005. Shaping the landscape: fire-grazer interactions in an African savanna. Ecol. Appl. 15, 96–109.

Baily, V.L., Pries, C.H., Lajtha, K., 2019. What do we know about soil carbon destabilization? Environ. Res. Lett. 14 (8), 083004.

Bond, W.J., Stevens, N., Midgley, G.F., Lehmann, C.E., 2019. The trouble with trees: afforestation plans for Africa. Trends Ecol. Evol. 34 (11), 963–965.

Breiman, L., 2001. Random forests. Mach. Learn. 45, 5–32. https://doi.org/10.1023/A:1010933404324.

Claverie, M., Vermote, E., 2014. NOAA Climate Data Record (CDR) of Leaf Area Index (LAI) and Fraction of Absorbed Photosynthetically Active Radiation (FAPAR), Version 4. [AVH15C1-LAI]. NOAA National Centers for Environmental Information.

Cramer, Michael D., Power, S.C., Belev, A., Gillson, L., Bond, W.J., Hoffman, M.T., Hedin, L.O., 2019a. Are forest-shrubland mosaics of the Cape Floristic Region an example of alternate stable states? Ecography 42, 717–729. https://doi.org/10.1111/ecog.03860.

Cramer, Michael D., Wootton, L.M., van Mazijk, R., Anthony Verboom, G., 2019b. New regionally modelled soil layers improve prediction of vegetation type relative to that based on global soil models. Divers. Distrib. 25, 1736–1750.

Delgado-Baquerizo, M., Eldridge, D.J., Maestre, F.T., Karunaratne, S.B., Trivedi, P., Reich, P.B., Singh, B.K., 2017. Climate legacies drive global soil carbon stocks in terrestrial ecosystems. Sci. Adv. 3, e1602008. https://doi.org/10.1126/sciadv.1602008.

Demattê, J.A.M., Safanelli, J.L., Poppiel, R.R., Rizzo, R., Silvero, N.E.Q., Mendes, W. de S., Bonfatti, B.R., Dotto, A.C., Salazar, D.F.U., Mello, F.A. de O., Paiva, A.F. da S., Souza, A.B., Santos, N.V. dos, Maria Nascimento, C., Mello, D.C. de, Bellinaso, H., Gonzaga Neto, L., Amorim, M.T.A., Resende, M.E.B. de, Vieira, J. da S., Queiroz, L.G. de, Gallo, B.C., Sayão, V.M., Lisboa, C.J. da S., 2020. Bare Earth's surface spectra as a proxy for soil resource monitoring. Sci. Rep. 10, 4461. https://doi.org/10.1038/s41598-020-61408-1.

Department of Environmental Affairs, 2015. National Terrestrial Carbon Sinks Assessment. Department of Environmental Affairs, Pretoria, South Africa.

Dieckow, J., Mielniczuk, J., Knicker, H., Bayer, C., Dick, D.P., Kögel-Knabner, I., 2007. Comparison of carbon and nitrogen determinations methods for samples of a paleudult subjected to no-till cropping systems. Sci. Agric. 64, 532–540. https://doi.org/10.1590/S0103-90162007000500011.

Eggleston, H.S., Buendia, L., Miwa, K., Ngara, T., Tanabe, K., 2006. 2006 IPCC Guidelines for National Greenhouse Gas Inventories.

Fairbanks, D., Thompson, M., Vink, D., Newby, T., Van den Berg, H., Everard, D., 2000. 2000. The South African land-cover characteristics database: a synopsis of the landscape. South Afr. J. Sci. 96.

Farr, T.G., Kobrick, M., 2000. Shuttle radar topography mission produces a wealth of data. EOS Trans. Am. Geophys. Union 81, 583–585. https://doi.org/10.1029/EO081i048p00583.

Fey, M., 2010. Soils of South Africa. Cambridge University Press, Cape Town, South Africa.

Friedlingstein, P., Jones, M.W., O'Sullivan, M., Andrew, R.M., Hauck, J., Peters, G.P., Peters, W., Pongratz, J., Sitch, S., Le Quéré, C., Bakker, D.C.E., Canadell, J.G., Ciais, P., Jackson, R.B., Anthoni, P., Barbero, L., Bastos, A., Bastrikov, V., Becker, M., Bopp, L., Buitenhuis, E., Chandra, N., Chevallier, F., Chini, L.P., Currie, K.I., Feely, R.A., Gehlen, M., Gilfillan, D., Gkritzalis, T., Goll, D.S., Gruber, N., Gutekunst, S., Harris, I., Haverd, V., Houghton, R.A., Hurtt, G., Ilyina, T., Jain, A.K., Joetzjer, E., Kaplan, J.O., Kato, E., Klein Goldewijk, K., Korsbakken, J.I., Landschützer, P., Lauvset, S.K., Lefèvre, N., Lenton, A., Lienert, S., Lombardozzi, D., Marland, G., McGuire, P.C., Melton, J.R., Metzl, N., Munro, D.R., Nabel, J.E.M.S., Nakaoka, S.-I., Neill, C., Omar, A.M., Ono, T., Peregon, A., Pierrot, D., Poulter, B., Rehder, G., Resplandy, L., Robertson, E., Rödenbeck, C., Séférian, R., Schwinger, J., Smith, N., Tans, P.P., Tian, H., Tilbrook, B., Tubiello, F.N., van der Werf, G.R., Wiltshire, A.J., Zaehle, S., 2019. Global carbon budget 2019. Earth Syst. Sci. Data 11, 1783–1838. https://doi.org/10.5194/essd-11-1783-2019.

Friedlingstein, P., O'Sullivan, M., Jones, M.W., Andrew, R.M., Hauck, J., Olsen, A., Peters, G.P., Peters, W., Pongratz, J., Sitch, S., Le Quéré, C., 2020. Global carbon budget 2020. Earth Syst. Sci. Data 12 (4), 3269–3340.

Goldstein, A., Turner, W.R., Spawn, S.A., Anderson-Teixeira, K.J., Cook-Patton, S., Fargione, J., Gibbs, H.K., Griscom, B., Hewson, J.H., Howard, J.F., Ledezma, J.C., Page, S., Koh, L.P., Rockström, J., Sanderman, J., Hole, D.G., 2020. Protecting irrecoverable carbon in Earth's ecosystems. Nat. Clim. Chang. 10, 287–295. https://doi.org/10.1038/s41558-020-0738-8.

Gomes, L.C., Faria, R.M., de Souza, E., Veloso, G.V., Schaefer, C.E.G.R., Filho, E.I.F., 2019. Modelling and mapping soil organic carbon stocks in Brazil. Geoderma 340, 337–350. https://doi.org/10.1016/j.geoderma.2019.01.007.

Gorelick, N., Hancher, M., Dixon, M., Ilyushchenko, S., Thau, D., Moore, R., 2017. Google Earth Engine: planetary-scale geospatial analysis for everyone. Remote Sens. Environ. 202, 18–27. https://doi.org/10.1016/j.rse.2017.06.031.

Griscom, B.W., Adams, J., Ellis, P.W., Houghton, R.A., Lomax, G., Miteva, D.A., Schlesinger, W.H., Shoch, D., Siikamäki, J.V., Smith, P., Woodbury, P., Zganjar, C., Blackman, A., Campari, J., Conant, R.T., Delgado, C., Elias, P., Gopalakrishna, T., Hamsik, M.R., Herrero, M., Kiesecker, J., Landis, E., Laestadius, L., Leavitt, S.M., Minnemeyer, S., Polasky, S., Potapov, P., Putz, F.E., Sanderman, J., Silvius, M., Wollenberg, E., Fargione, J., 2017. Natural climate solutions. Proc. Natl. Acad. Sci. 114, 11645–11650. https://doi.org/10.1073/pnas.1710465114.

Guevara, M., Arroyo, C., Brunsell, N., Cruz, C.O., Domke, G., Equihua, J., Etchevers, J., Hayes, D., Hengl, T., Ibelles, A., Johnson, K., de Jong, B., Libohova, Z., Llamas, R., Nave, L., Ornelas, J.L., Paz, F., Ressl, R., Schwartz, A., Victoria, A., Wills, S., Vargas, R., 2020. Soil organic carbon across Mexico and the conterminous United States (1991–2010). Glob. Biogeochem. Cycles 34, e2019GB006219. https://doi.org/10.1029/2019GB006219.

Guyon, I., Weston, J., Barnhill, S., Vapnik, V., 2002. Gene selection for cancer classification using support vector machines. Mach. Learn. 46, 389–422.

Hengl, T., MacMillan, R.A., 2019. Predictive Soil Mapping With R. OpenGeoHub foundation, Wageningen, the Netherlands.

Hengl, T., Mendes de Jesus, J., Heuvelink, G.B., Ruiperez Gonzalez, M., Kilibarda, M., Blagotić, A., Shangguan, W., Wright, M.N., Geng, X., Bauer-Marschallinger, B., 2017. SoilGrids250m: global gridded soil information based on machine learning. PLoS ONE 12, e0169748.

Hengl, T., Miller, M., Križan, J., Kilibarda, M., 2020. iSDAsoil: Soil Total Carbon for Africa Predicted at 30 m Resolution at 0–20 and 20–50 cm Depths. https://doi.org/10.5281/zenodo.4088064.

Heuvelink, G.B.M., Angelini, M.E., Poggio, L., Bai, Z., Batjes, N.H., van den Bosch, R., Bossio, D., Estella, S., Lehmann, J., Olmedo, G.F., Sanderman, J., 2020. Machine learning in space and time for modelling soil organic carbon change. Eur. J. Soil Sci. https://doi.org/10.1111/ejss.12998 n/a.

Hijmans, R.J., Cameron, S.E., Parra, J.L., Jones, P.G., Jarvis, A., 2005. Very high resolution interpolated climate surfaces for global land areas. Int. J. Climatol. 25, 1965–1978. https://doi.org/10.1002/joc.1276.

Hoffman, M.T., Todd, S., 2000. A national review of land degradation in South Africa: the influence of biophysical and socio-economic factors. J. South. Afr. Stud. 26, 743–758. https://doi.org/10.1080/713683611.

Holden, C.E., Woodcock, C.E., 2016. An analysis of Landsat 7 and Landsat 8 underflight data and the implications for time series investigations. Remote Sens. Environ. 185, 16–36. https://doi.org/10.1016/j.rse.2016.02.052.

Hopper, S.D., Lambers, H., 2009. Darwin as a plant scientist: a Southern Hemisphere perspective. Trends Plant Sci. 14, 421–435. https://doi.org/10.1016/j.tplants.2009.06.004.

Hopper, S.D., Silveira, F.A.O., Fiedler, P.L., 2016. Biodiversity hotspots and Ocbil theory. Plant Soil 403, 167–216. https://doi.org/10.1007/s11104-015-2764-2.

Houghton, R., 2007. Balancing the global carbon budget. Annu. Rev. Earth Planet. Sci. 35, 313–347.

Huang, J., Minasny, B., McBratney, A.B., Padarian, J., Triantafilis, J., 2018. The location- and scale- specific correlation between temperature and soil carbon sequestration across the globe. Sci. Total Environ. 615, 540–548. https://doi.org/10.1016/j.scitotenv.2017.09.136.

IUSS Working Group WRB, 2015. World reference base for soil resources 2014, update 2015: international soil classification system for naming soils and creating legends for soil maps. World Soil Resour. Rep. No 106 192.

Jobbágy, E.G., Jackson, R.B., 2000. The vertical distribution of soil organic carbon and its relation to climate and vegetation. Ecol. Appl. 10 (2), 423–436.

Jones, M.W., Santín, C., van der Werf, G.R., Doerr, S.H., 2019. Global fire emissions buffered by the production of pyrogenic carbon. Nat. Geosci. 12, 742–747. https://doi.org/10.1038/s41561-019-0403-x.

Khaledian, Y., Miller, B.A., 2020. Selecting appropriate machine learning methods for digital soil mapping. Appl. Math. Model. 81, 401–418. https://doi.org/10.1016/j.apm.2019.12.016.

Kleber, M., Nico, P.S., Plante, A., Filley, T., Kramer, M., Swanston, C., Sollins, P., 2011. Old and stable soil organic matter is not necessarily chemically recalcitrant: implications for modeling concepts and temperature sensitivity. Glob. Chang. Biol. 17, 1097–1107.

Knorr, W., Prentice, I.C., House, J.I., Holland, E.A., 2005. Long-term sensitivity of soil carbon turnover to warming. Nature 433, 298–301. https://doi.org/10.1038/nature03226.

Lal, R., 2004. Soil carbon sequestration impacts on global climate change and food security. Science 304, 1623–1627. https://doi.org/10.1126/science.1097396.

Lamichhane, S., Kumar, L., Wilson, B., 2019. Digital soil mapping algorithms and covariates for soil organic carbon mapping and their implications: a review. Geoderma. https://doi.org/10.1016/j.geoderma.2019.05.031.

Le Quéré, C., Andrew, R.M., Friedlingstein, P., Sitch, S., Pongratz, J., Manning, A.C., Korsbakken, J.I., Peters, G.P., Canadell, J.G., Jackson, R.B., Boden, T.A., Tans, P.P., Andrews, O.D., Arora, V.K., Bakker, D.C.E., Barbero, L., Becker, M., Betts, R.A., Bopp, L., Chevallier, F., Chini, L.P., Ciais, P., Cosca, C.E., Cross, J., Currie, K., Gasser, T., Harris, I., Hauck, J., Haverd, V., Houghton, R.A., Hunt, C.W., Hurtt, G., Ilyina, T., Jain, A.K., Kato, E., Kautz, M., Keeling, R.F., Klein Goldewijk, K., Körtzinger, A., Landschützer, P., Lefèvre, N., Lenton, A., Lienert, S., Lima, I., Lombardozzi, D., Metzl, N., Millero, F., Monteiro, P.M.S., Munro, D.R., Nabel, J.E.M.S., Nakaoka, S., Nojiri, Y., Padin, X.A., Peregon, A., Pfeil, B., Pierrot, D., Poulter, B., Rehder, G., Reimer, J., Rödenbeck, C., Schwinger, J., Séférian, R., Skjelvan, I., Stocker, B.D., Tian, H., Tilbrook, B., Tubiello, F.N., van der Laan-Luijkx, I.T., van der Werf, G.R., van Heuven, S., Viovy, N., Vuichard, N., Walker, A.P., Watson, A.J., Wiltshire, A.J., Zaehle, S., Zhu, D., 2018. Global carbon budget 2017. Earth Syst. Sci. Data 10, 405–448. https://doi.org/10.5194/essd-10-405-2018.

Lechmere-Oertel, R.G., Kerley, G.I.H., Cowling, R.M., 2005. Patterns and implications of transformation in semi-arid succulent thicket, South Africa. J. Arid Environ. 62 (3), 459–474.

Lloyd, J.W., Van den Berg, E.C., Palmer, A.R., 2002. Patterns of transformation and degradation in the thicket biome, South Africa. TERU Report. 39, p. 86.

Marschner, B., Brodowski, S., Dreves, A., Gleixner, G., Gude, A., Grootes, P.M., Hamer, U., Heim, A., Jandl, G., Ji, R., Kaiser, K., Kalbitz, K., Kramer, C., Leinweber, P., Rethemeyer, J., Schäffer, A., Schmidt, M.W.I., Schwark, L., Wiesenberg, G.L.B., 2008. How relevant is recalcitrance for the stabilization of organic matter in soils? J. Plant Nutr. Soil Sci. 171, 91–110. https://doi.org/10.1002/jpln.200700049.

Mattina, D., Erdogan, H., Wheeler, I., Crossman, N., Cumani, R., 2018. Default data: methods and interpretation. A Guidance Document for the 2018 UNCCD Reporting. Presented at the United Nations Convention to Combat Desertification (UNCCD).

McGuire, A.D., Melillo, J.M., Kicklighter, D.W., Joyce, L.A., 1995. Equilibrium responses of soil carbon to climate change: empirical and process-based estimates. J. Biogeogr. 785–796.

Mills, A.J., Cowling, R.M., 2006. Rate of carbon sequestration at two thicket restoration sites in the Eastern Cape, South Africa. Restor. Ecol. 14 (1), 38–49.

Mills, A.J., Cowling, R.M., 2014. How fast can carbon be sequestered when restoring degraded subtropical thicket? Restor. Ecol. 22 (5), 571–573.

Mills, A., Cowling, R., Fey, M., Kerley, G., Donaldson, J., Lechmere-Oertel, R., Sigwela, A., Skowno, A., Rundel, P., 2005. Effects of goat pastoralism on ecosystem carbon storage in semiarid thicket, Eastern Cape, South Africa. Austral Ecol. 30, 797–804.

Mills, A.J., Fey, M.V., 2004. Declining soil quality in South Africa: effects of land use on soil organic matter and surface crusting. South Afr. J. Plant Soil 21, 388–398. https://doi.org/10.1080/02571862.2004.10635071.

Mills, A.J., der Vyver, M.V., Gordon, I.J., Patwardhan, A., Marais, C., Blignaut, J., Sigwela, A., Kgope, B., 2015. Prescribing innovation within a large-scale restoration programme in degraded subtropical thicket in South Africa. Forests 6, 4328–4348.

Mucina, L., Rutherford, M.C., Powrie, L.W., 2018. The Vegetation Map of South Africa, Lesotho and Swaziland. South African National Biodiversity, Cape Town.

Myers, N., Mittermeier, R.A., Mittermeier, C.G., da Fonseca, G.A.B., Kent, J., 2000. Biodiversity hotspots for conservation priorities. Nature 403, 853–858. https://doi.org/10.1038/35002501.

Nayak, A.K., Rahman, M.M., Naidu, R., Dhal, B., Swain, C.K., Nayak, A.D., Tripathi, R., Shahid, M., Islam, M.R., Pathak, H., 2019. Current and emerging methodologies for estimating carbon sequestration in agricultural soils: a review. Sci. Total Environ. 665, 890–912. https://doi.org/10.1016/j.scitotenv.2019.02.125.

Newton, I.P., Knight, R.S., 2005. The use of a 60-year series of aerial photographs to assess local agricultural transformations of West Coast Renosterveld, an endangered South African vegetation type. S. Afr. Geogr. J. 87, 18–27.

Padarian, J., Minasny, B., McBratney, A.B., 2020. Machine learning and soil sciences: a review aided by machine learning tools. SOIL 6, 35–52. https://doi.org/10.5194/soil-6-35-2020.

Pellegrini, A.F.A., Ahlström, A., Hobbie, S.E., Reich, P.B., Nieradzik, L.P., Staver, A.C., Scharenbroch, B.C., Jumpponen, A., Anderegg, W.R.L., Randerson, J.T., Jackson, R.B., 2018. Fire frequency drives decadal changes in soil carbon and nitrogen and ecosystem productivity. Nature 553, 194–198. https://doi.org/10.1038/nature24668.

Pettorelli, N., Vik, J.O., Mysterud, A., Gaillard, J.-M., Tucker, C.J., Stenseth, N.Chr, 2005. Using the satellite-derived NDVI to assess ecological responses to environmental change. Trends Ecol. Evol. 20, 503–510. https://doi.org/10.1016/j.tree.2005.05.011.

Piñeiro, G., Perelman, S., Guerschman, J.P., Paruelo, J.M., 2008. How to evaluate models: observed vs. predicted or predicted vs. observed? Ecol. Model. 216, 316–322.

Power, S.C., Verboom, G.A., Bond, W.J., Cramer, M.D., 2017. Environmental correlates of biome-level floristic turnover in South Africa. J. Biogeogr. 44, 1745–1757. https://doi.org/10.1111/jbi.12971.

Ramifehiarivo, N., Brossard, M., Grinand, C., Andriamananjara, A., Razafimbelo, T., Rasolohery, A., Razafimahatratra, H., Seyler, F., Ranaivoson, N., Rabenarivo, M., Albrecht, A., Razafindrabe, F., Razakamanarivo, H., 2017. Mapping soil organic carbon on a national scale: towards an improved and updated map of Madagascar. Geoderma Reg., Digital Soil Mapping Across the Globe. 9, pp. 29–38. https://doi.org/10.1016/j.geodrs.2016.12.002.

Reisser, M., Purves, R.S., Schmidt, M.W.I., Abiven, S., 2016. Pyrogenic carbon in soils: a literature-based inventory and a global estimation of its content in soil organic carbon and stocks. Front. Earth Sci. 4. https://doi.org/10.3389/feart.2016.00080.

Robinson, T.P., Wint, G.R.W., Conchedda, G., Boeckel, T.P.V., Ercoli, V., Palamara, E., Cinardi, G., D'Aietti, L., Hay, S.I., Gilbert, M., 2014. Mapping the global distribution of livestock. PLoS ONE 9, e96084. https://doi.org/10.1371/journal.pone.0096084.

Roy, D.P., Kovalskyy, V., Zhang, H.K., Vermote, E.F., Yan, L., Kumar, S.S., Egorov, A., 2016. Characterization of Landsat-7 to Landsat-8 reflective wavelength and normalized difference vegetation index continuity. Remote Sens. Environ. 185, 57–70. https://doi.org/10.1016/j.rse.2015.12.024.

Rumpel, C., Amiraslani, F., Chenu, C., Garcia Cardenas, M., Kaonga, M., Koutika, L.-S., Ladha, J., Madari, B., Shirato, Y., Smith, P., Soudi, B., Soussana, J.-F., Whitehead, D., Wollenberg, E., 2020. The 4p1000 initiative: opportunities, limitations and challenges for implementing soil organic carbon sequestration as a sustainable development strategy. Ambio 49, 350–360. https://doi.org/10.1007/s13280-019-01165-2.

Sanderman, J., Hengl, T., Fiske, G.J., 2017. Soil carbon debt of 12,000 years of human land use. Proc. Natl. Acad. Sci. 114, 9575–9580. https://doi.org/10.1073/pnas.1706103114.

Scholes, R., Montanarella, L., Brainich, E., Barger, N., ten Brink, B., Cantele, M., Erasmus, B., Fisher, J., Gardner, T., Holland, T., 2018. IPBES (2018): Summary for Policymakers of the Assessment Report on Land Degradation and Restoration of the Intergovernmental Science-policy Platform on Biodiversity and Ecosystem Services.

Schulze, R.E., Schütte, S., 2020. Mapping soil organic carbon at a terrain unit resolution across South Africa. Geoderma 373, 114447. https://doi.org/10.1016/j.geoderma.2020.114447.

Sen, P.K., 1968. Estimates of the regression coefficient based on Kendall's tau. J. Am. Stat. Assoc. 63, 1379–1389. https://doi.org/10.1080/01621459.1968.10480934.

Sigwela, A.M., Kerley, G.I.H., Mills, A.J., Cowling, R.M., 2009. The impact of browsing-induced degradation on the reproduction of subtropical thicket canopy shrubs and trees. S. Afr. J. Bot. 75 (2), 262–267.

Skowno, A.L., Thompson, M.W., Hiestermann, J., Ripley, B., West, A.G., Bond, W.J., 2017. Woodland expansion in South African grassy biomes based on satellite observations (1990–2013): general patterns and potential drivers. Glob. Chang. Biol. 23, 2358–2369. https://doi.org/10.1111/gcb.13529.

Smith, P., Soussana, J.-F., Angers, D., Schipper, L., Chenu, C., Rasse, D.P., Batjes, N.H., van Egmond, F., McNeill, S., Kuhnert, M., Arias-Navarro, C., Olesen, J.E., Chirinda, N., Fornara, D., Wollenberg, E., Álvaro-Fuentes, J., Sanz-Cobena, A., Klumpp, K., 2020. How to measure, report and verify soil carbon change to realize the potential of soil carbon sequestration for atmospheric greenhouse gas removal. Glob. Chang. Biol. 26, 219–241. https://doi.org/10.1111/gcb.14815.

Soil Classification Working Group, 1991. Soil classification: a taxonomic system for South Africa. Mem. Agric. Nat. Resour. South Afr. 15, 1–262.

SoilGrids, 2019. Global gridded soil information [WWW Document]. URL isric.org/explore/soilgrids (accessed (accessed 7.24.20).

de Sousa, L.M., Poggio, L., Batjes, N.H., Heuvelink, G.B.M., Kempen, B., Riberio, E., Rossiter, D., 2020. SoilGrids 2.0: producing quality-assessed soil information for the globe. Soil Discuss., 1–37 https://doi.org/10.5194/soil-2020-65.

Statistics South Africa, 2020. Census of commercial agriculture 2017. Financial and production statistics. (No. 11- 02– 01 (2017)). Statistics South Africa.

Stockmann, U., Padarian, J., McBratney, A., Minasny, B., de Brogniez, D., Montanarella, L., Hong, S.Y., Rawlins, B.G., Field, D.J., 2015. Global soil organic carbon assessment. Glob. Food Sec. 6, 9–16. https://doi.org/10.1016/j.gfs.2015.07.001.

Theobald, D.M., Harrison-Atlas, D., Monahan, W.B., Albano, C.M., 2015. Ecologically-relevant maps of landforms and physiographic diversity for climate adaptation planning. PLoS ONE 10, e0143619.

Thompson, M., 2018. South African National Land-cover 2018 Report & Accuracy Assessment. GeoTerraImage, Pretoria.

Tucker, C.J., 1979. Red and photographic infrared linear combinations for monitoring vegetation. Remote Sens. Environ. 8, 127–150. https://doi.org/10.1016/0034-4257(79)90013-0.

Venter, Z.S., Hawkins, H.-J., Cramer, M.D., 2017. Implications of historical interactions between herbivory and fire for rangeland management in African savannas. Ecosphere 8. https://doi.org/10.1002/ecs2.1946.

Venter, Z.S., Cramer, M.D., Hawkins, H.-J., 2018. Drivers of woody plant encroachment over Africa. Nat. Commun. 9. https://doi.org/10.1038/s41467-018-04616-8.

Walkley, A., Black, I.A., 1934. An examination of the Degtjareff method for determining soil organic matter, and a proposed modification of the chromic acid titration method. Soil Sci. 37, 29–38.

Wiesmeier, M., Poeplau, C., Sierra, C.A., Maier, H., Frühauf, C., Hübner, R., Kühnel, A., Spörlein, P., Geuß, U., Hangen, E., Schilling, B., von Lützow, M., Kögel-Knabner, I., 2016. Projected loss of soil organic carbon in temperate agricultural soils in the 21

st century: effects of climate change and carbon input trends. Sci. Rep. 6, 32525. https://doi.org/10.1038/srep32525.

Wilcox, R.R., 2010. Fundamentals of Modern Statistical Methods: Substantially Improving Power and Accuracy. Springer.

Willmott, C.J., 1981. On the validation of models. Phys. Geogr. 2, 184–194.

Xiao, J., Chevallier, F., Gomez, C., Guanter, L., Hicke, J.A., Huete, A.R., Ichii, K., Ni, W., Pang, Y., Rahman, A.F., Sun, G., Yuan, W., Zhang, L., Zhang, X., 2019. Remote sensing of the terrestrial carbon cycle: a review of advances over 50 years. Remote Sens. Environ. 233, 111383. https://doi.org/10.1016/j.rse.2019.111383.

Zhou, Y., Hartemink, A.E., Shi, Z., Liang, Z., Lu, Y., 2019. Land use and climate change effects on soil organic carbon in North and Northeast China. Sci. Total Environ. 647, 1230–1238. https://doi.org/10.1016/j.scitotenv.2018.08.016.

Zhu, Z., 2017. Change detection using landsat time series: a review of frequencies, preprocessing, algorithms, and applications. ISPRS J. Photogramm. Remote Sens. 130, 370–384. https://doi.org/10.1016/j.isprsjprs.2017.06.013.

Zuur, A.F., Ieno, E.N., Elphick, C.S., 2010. A protocol for data exploration to avoid common statistical problems. Methods Ecol. Evol. 1, 3–14. https://doi.org/10.1111/j.2041-210X.2009.00001.x.